irradiation. The position of the second peak is similar in the second and third samples and allows an estimate to be made of the molecular weight of the micelles.

From a calibration of the column with a set of monodisperse polystyrene samples, one finds that the viscosity-average molecular weight of the free polymer molecules is 43 000; that of the micelles is abut 350 000. The average number of macromolecules per multimolecular micelle is therefore 350:43 = 8. This value is in good agreement with the quantum yield of cross-link formation, $\Phi = 9$, measured in films of the same material cast from THF solution.[1] It will be recalled that the quantum yield of intermolecular cross-link formation measures in effect the number of polymer chains taking part in the average diacetylene stack of the solid film.

From these data and from the composition of the polymer, the volume of the micelle core is estimated to be of the order of 1×10^{-18} cm^3, corresponding to an inner core diameter of about 100 Å. The overall micelle volume is estimated at 6×10^{-18} cm^3, corresponding to an outer micelle diameter of 180 Å.

Registry No. (HDI)(HOCH$_2$C≡CC≡CCH$_2$OH)(CL) (copolymer), 109960-52-3.

References and Notes

(1) Liang, R. C.; Reiser, A. *J. Imag. Sci.* **1986**, *30*, 69.
(2) Liang, R. C.; Lai, W. Y. F.; Reiser, A. *Macromolecules* **1986**, *19*, 1685.
(3) Lai, W. Y. F. Nourbakhsh, private communication, 1986.
(4) Gallot, B. *Adv. Polym. Sci.* **1978**, *29*, 87.
(5) Krause, S. *J. Phys. Chem.* **1964**, *68*, 1948.
(6) Kotaka, T.; Tanaka, T.; Inagaki, H. *Polym. J.* **1972**, *3*, 327.
(7) Tuzar, Z.; Kratochvil, P. *Makromol. Chem.* **1972**, *160*, 301.
(8) Shibayama, M.; Hashimoto, T.; Hasegawa, H.; Kawai, H. *Macromolecules* **1983**, *16*, 1427, 1437. Shibayama, M.; Hashimoto, T.; Kawai, H. *Macromolecules* **1983**, *16*, 1434. Hashimoto, T. *Macromolecules* **1987**, *20*, 465 and references therein.
(9) Noolandi, J.; Hong, K. M. *Macromolecules* **1983**, *16*, 1443.
(10) Leibler, L. *Macromolecules* **1980**, *13*, 1602.
(11) Leibler, L.; Orland, H.; Wheeler, J. C. *J. Chem. Phys.* **1983**, *79*, 3550.
(12) Zin, W. Ch.; Roe, R. J. *Macromolecules* **1984**, *17*, 183.
(13) Roe, R. J.; Zin, W. Ch. *Macromolecules* **1984**, *17*, 189.
(14) Tuzar, Z.; Plestil, J.; Konak, C.; Hlavata, D.; Sikora, A. *Makromol. Chem.* **1983**, *184*, 2111.
(15) Elias, H.-G. *J. Macromol. Sci. Chem.* **1973**, *A-7*, 601.
(16) Liang, R. C.; Reiser, A. *J. Polym. Sci., Polym. Chem. Ed.* **1987**, *25*, 451.
(17) Sixl, H. In *Polydiacetylenes*; Cantow, H.-J., Ed.; Springer: Berlin, 1984; p 49.
(18) Spacek, P.; Kubin, M. *J. Appl. Polym. Sci.* **1985**, *30*, 143.
(19) Chang, L. P.; Morawetz, H. *Macromolecules* **1987**, *20*, 428.

Polycondensation of Methyltrimethoxysilane

K. A. Smith

Research & Development Center, Corporate Research & Development, General Electric Company, Schenectady, New York 12301.

Received September 26, 1986

ABSTRACT: Kinetics of the hydrolysis and self-condensation of methyltrimethoxysilane in organic–water (acetone-d_6 or CD_3CN) solvent systems were studied. The specific acid-catalyzed hydrolysis was found to be first order in substrate. By ^{29}Si NMR techniques, condensation was monitored and modeled by a set of propagation and condensation reactions. The solution to this set of equations indicates that hydrolysis of methyltrimethoxysilane and condensation of partially hydrolyzed methyltrimethoxysilane have competitive rates. Reactions between condensed species are on the average 17 times slower than condensations involving partially hydrolyzed methyltrimethoxysilane. Further characterization of condensation was attempted by using a statistical model with kinetic constraints. This approach was shown, in the limit reached by assuming diffusion between all sites, to be the same description obtained by the finite difference solution to a set of rate expressions for propagation and condensation processes. The molecular weight distribution as a function of the extent of reaction, as well as the gel point, was deduced from the model, and the dependence of the latter on attributes of the model is discussed.

Introduction

The hydrolysis and condensation chemistry of alkoxysilanes (or silanols derived from them) has been studied extensively.[1-4] The more quantitative investigations have, in general, been concerned with hydrolysis[1] owing to the relative simplicity of this process compared to condensation, particularly polycondensation of di-, or tri-, or tetraalkoxysilanes. This is not to imply that descriptions of the polycondensation chemistry of these systems have not appeared in the literature. Indeed, ceramic literature contains several examples of studies of tetraalkoxysilane hydrolysis and condensation.[2] Although analogous work on difunctional compounds has been reported,[3] comparable studies of trialkoxysilanes are rare.[4]

$$n\mathrm{CH_3Si(OCH_3)_3} + 1.5n\mathrm{H_2O} \xrightarrow{\mathrm{H^+}} \text{polysiloxanes} + 3n\mathrm{CH_3OH} \quad (1)$$

where for complete reaction, polysiloxanes = $[CH_3SiO_{1.5}]_n$

The role of trialkoxysilanes in resin synthesis, in addition to their place in elastomer technology, led to the experiments described herein. The concerns of relative hydrolysis and condensation rates (eq 1) of methyltrimethoxysilane (MTMS), the simplest alkyltrialkoxysilane, as well as the general question of how to model this polycondensation process, were foremost in our minds and are the focal points of this study.

Results and Discussion

Hydrolysis Studies. The hydrolysis of MTMS catalyzed by *p*-toluenesulfonic acid (*p*-TSA) in acetone was followed by GC analysis, as well as ^{1}H NMR spectroscopy. These experiments found hydrolysis to be first order in substrate under conditions of excess water (11 equiv)—plots of ln [MTMS] versus time being linear ($r > 0.99$) for greater than three half-lives. This dependence, in conjunction with the absence of dimer 1,1,3,3-tetramethoxy-1,3-dimethyldisiloxane (1) as a product, suggests that MTMS does not undergo a competitive condensation reaction with initially formed hydrolysis products. An additional verification of this conclusion was the demonstration that 1 hydrolyzes 16 times more slowly than

0024-9297/87/2220-2514$01.50/0

Table I
Catalytic Rate Constants as a Function of Brønsted Catalyst

catalyst	k_{cat}, M^{-2} s^{-1}	pK_a[a]
p-TSA	7 ± 2	−1.3
CF_3CO_2H	0.34 ± 0.10	0.0
CH_3CO_2H	1.6×10^{-2}	4.76

[a] In water, ref 6.

MTMS and thus, if formed under the reaction conditions, would have been observed. By GC analysis few products of the hydrolysis/condensation are observed. Presumably the presence of silanol functionality in the products[5] coupled with their rather high molecular weight precludes using this analytical technique. In addition, since ^1H NMR methods could not distinguish the various products formed, ^{29}Si NMR spectroscopy was employed to study condensation (vide infra).

A brief survey of acid catalysts (Tabe I) indicates the presence of either general-acid or general-base catalysis as suggested by the anomalously rapid k_{obsd} for the acetic acid catalyzed hydrolysis. This conclusion rests on the assumption that the relative pK_as of the acids as determined in water hold as one goes to the acetone–water system. General-base catalysis has been documented in several related hydrolysis studies and presumably is an additional term of consequence in the acetic acid example.[1a] In the experiments reported in this paper, strong acids such as *p*-TSA were used, and the disappearance of substrate could be described by a single, specific-acid term, i.e.,

$$d[MTMS]/dt = -k_{obsd}[MTMS][H^+]$$

Catalyst dependence was examined over a narrow range of catalyst concentrations, $[H^+] = 10^{-3}$ to 10^{-5} M. Because of the limitations of GC analysis (particularly the finite cycle times between samples), it was not possible to go to higher acid concentrations. On the low concentration side, as these were unbuffered systems, maintenance of constant acidity[7] over the course of the reaction was problematic. Within the narrow range noted above the catalyst order was 1.0 ± 0.1.

Condensation Studies

Observations. ^{29}Si NMR spectroscopy was used to follow the condensation of MTMS. This technique has been applied to the study of kinetics or product distributions in silicate systems[2a-d] and for qualitative information in studies of trifunctional silicon systems.[4b] In the case of MTMS there is good separation between starting material and subsequent condensation products (see Figure 1 or 2), thus one is limited only by acquisition time for the spectra (see Experimental Section). Naturally, a significant difference between the GC experiments described above and the NMR studies was the higher concentration of MTMS required in the NMR investigations (1.3–3.2 M compared to 0.1–0.2 M). It should be noted that 1 was not detected as a substantial product even at [MTMS] = 2.5 M and less than 2 equiv of H_2O. At amounts of water less than stoichiometric with respect to MTMS (i.e. < 1.5 equiv), unreacted MTMS is found along with condensation products. It is worthwhile to compare these observations with those of Lin and Basil[2d] in their studies of tetraethoxysilane (TEOS) hydrolysis and condensation. They suggest that the partially hydrolyzed species are more reactive toward condensation as the number of hydroxy ligands increases. They also do not observe the dimer (in their case 1,1,1,3,3,3-hexaethoxy-1,3-disiloxane) during the hydrolysis and condensation of TEOS.

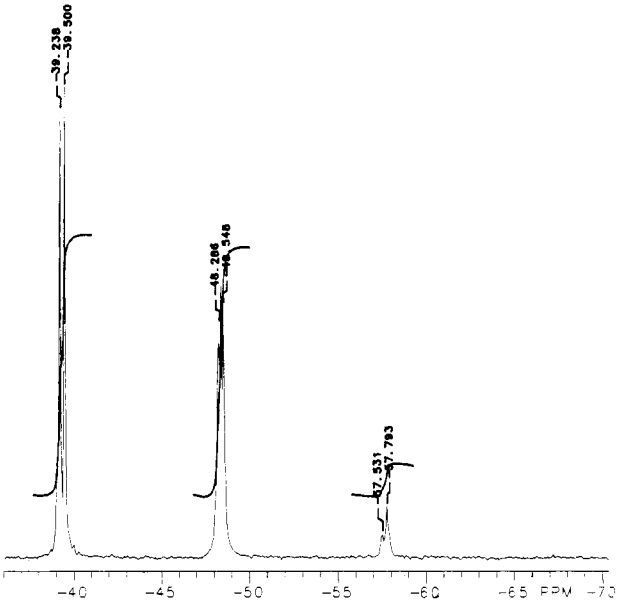

Figure 1. ^{29}Si NMR spectra of MTMS in CD_3CN/D_2O in the presence of *p*-TSA (calculated pH 2.8): $[D_2O]$ = 2.42 M; [MTMS] = 3.25 M obtained after 1 h.

Scheme I

$$2\,M^* \xrightarrow{k_1} 2\,END$$
$$M^* + END \xrightarrow{k_2} END + MID$$
$$M^* + MID \xrightarrow{k_3} END + SAT$$
$$2\,END \xrightarrow{k_4} 2\,MID$$
$$END + MID \xrightarrow{k_5} MID + SAT$$
$$2\,MID \xrightarrow{k_6} 2\,SAT$$

At some intermediate time in the reaction of 0.75 equiv of deuterium oxide with MTMS (calculated pH 2.8), the spectrum (Figure 1) shows unreacted MTMS (−39.5 ppm), what is presumably partially hydrolyzed MTMS (−37 ppm), and condensed products—groups of resonances at −48 and −57 ppm.

Figure 2 shows spectra of MTMS hydrolyzing and condensing over time.[8] The concentration of reagents is listed in the legend. Qualitatively, one observes rapid disappearance of starting material and formation of condensed products - primarily silicons bearing one and two siloxy groups. In the later stages of the reaction one notes the disappearance of silicons bearing only one siloxy ligand (so-called END groups, see below) and the eventual presence of only those silicons having two or three siloxy ligands.

In the NMR runs the functionality could be differentiated only to the extent that silicons bearing none to three siloxy groups were distinguishable. That is, whether a silicon bore, in addition to siloxy ligands, alkoxy versus hydroxy groups could not be determined. These types of silicon species along with their chemical shifts are indicated in Figures 1 and 2. Their assignments are based on literature precedence.[9]

With these data the reactions listed in Scheme I were considered to be general and sufficient to model the processes observed in the NMR experiment. The monomer, M*, is an "activated", partially hydrolyzed MTMS molecule, whose proposed intermediacy stems from the hydrolysis kinetics. The terms END, MID, and SAT refer to silicon bearing one, two, and three siloxy groups, respectively. Those reactions involving monomers are simple

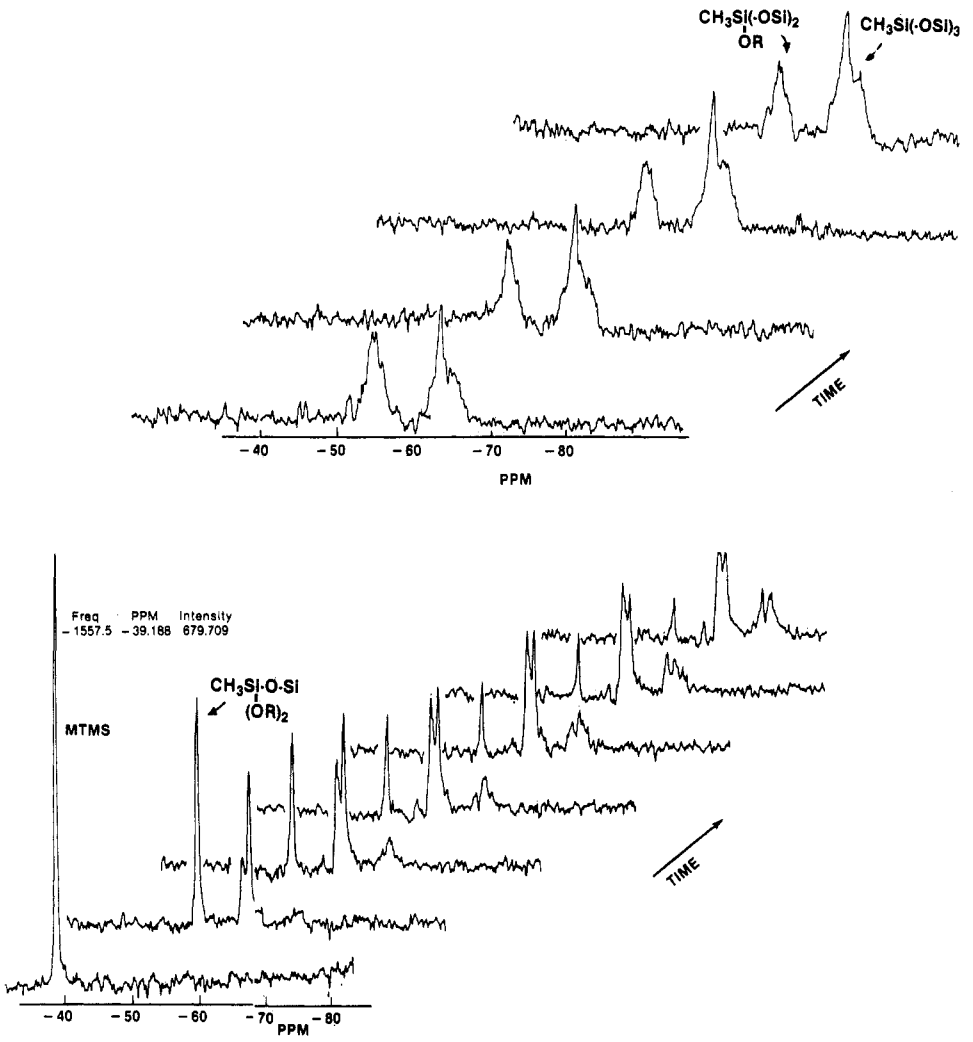

Figure 2. ^{29}Si NMR spectra of MTMS in acetone-d_6/D_2O in the presence of *p*-TSA (calculated pH 2.85); $[MTMS]_i$ = 2.87 M; $[D_2O]_i$ = 8.3 M obtained over time.

Scheme II

$$CH_3Si(OCH_3)_3 \underset{-H^+}{\overset{+H^+}{\rightleftharpoons}} CH_3Si(OCH_3)_2 \xrightarrow[-CH_3OH]{+H_2O \text{ (slow step)}} \underset{H^+OCH_3}{CH_3Si(OCH_3)_2}$$

$$\underset{OH}{CH_3Si(OCH_3)_2} + H^+ \xrightarrow{\text{subsequent hydrolysis steps}} CH_3Si(OH)_3$$

propagation steps, while reactions involving other species, END and MID, are simply termed "condensation" reactions. This treatment reduces the large manifold of reactants and products to a tractable system based on functionality. Implicitly, the mechanism of condensation is assumed to resemble that for hydrolysis (Scheme II),[1b] namely, a fast protonation equilibrium involving M* which then undergoes a reaction with silanol functionality rather than water. The fundamental condensation reaction is between a silanol and a silicon bearing at least one hydroxyl group (eq 2), while the leaving group is either

$$CH_3Si(OR)_2OH + CH_3Si(OCH_3)_x(OH)_{3-x} \xrightarrow{H^+} CH_3Si(OR)_2OSi(OR)_2CH_3 + CH_3OH \quad x = 0\text{–}2;\ R = H, CH_3, Si \quad (2)$$

methanol or water. No studies in the literature clarify how large a rate difference one would anticipate for either scenario. In any event, in the model described herein the two possibilities are indistinguishable.

Some General Considerations. Characterization of gelation and condensation processes involving multifunctional species has a long history beginning with the initial enunciation of a statistical model by Flory[10] and, independently, Stockmayer.[11] With time, the question has been refined to whether gelation is more aptly described by the Flory–Stockmayer (F–S) theory and other continuum models[12,13] or by bond production on a three-dimensional lattice.[14a] The general issue of whether gelation, as a critical phenomenon, belongs to the same universality class as other critical processes has also been addressed through lattice models.[14b–d]

In a vaguely related vein, Monte Carlo simulations of reaction kinetics have been reported by various workers.[15] These treatments are considered to be alternative descriptions of evolving systems compared to those derived from differential equations. In general, the two problems, kinetics and models of polycondensation, have not been examined in concert. Only recently have investigators noted that kinetic considerations may place a model into a completely different universality class from those in which these factors are neglected.[14b]

Against this background, the investigations of siloxane formation arising from MTMS hydrolysis and condensation promoted by a proton catalyst (eq 1) led to an effort to apply kinetic constraints to a statistical model and elucidate aspects of polycondensation, e.g., molecular weight distributions and critical parameters, not readily accessible from a differential equation description. Some

Table II
Scalars from Lattice Model in Comparison with Relative k_n from Difference Equations

	rel s_n		
n	CN = 26	CN = 8K[a]	rel k_n[b]
1	11.1	428	460
2	8.6	330	667
3	3.6	71	100
4	4.5	46	50
5	1.1	4.3	19
6	1.0	1.0	1.0

[a] $\bar{s}_{prop} = 16\bar{s}_{cond}$, where $\bar{s}_{prop} \equiv {}^1/_3\sum_{i=1}^{3} s_i$ and $\bar{s}_{cond} \equiv {}^1/_3\sum_{i=4}^{6} s_i$. [b] $\bar{k}_{prop} = 17\bar{k}_{cond}$.

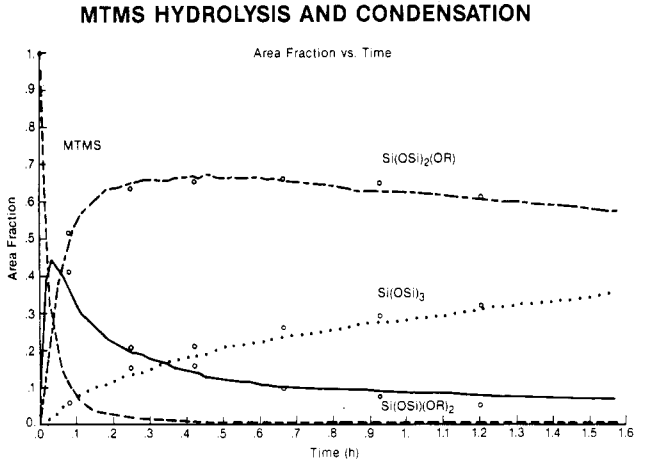

Figure 3. Fit to experimental data (open circles) by using lattice model with CN = 26.

implications of this approach are discussed.

Lattice Model. The lattice model used to fit the NMR data consists of a cubic array with periodic boundary conditions. At initial time the array is populated with M*, so that one is beginning the simulation at a point where all reacting centers have been formed and none have yet reacted. These initial conditions correspond to a situation where a relatively large excess of water is present.

Monte Carlo techniques were employed to develop the array over time, with criteria for bond formation arising from the nature of the reacting centers. Thus, one randomly selects some lattice point and then randomly selects another point in the neighborhood of the first. A probability factor for bond formation occurring between the two centers is compared to a randomly generated scalar and then, depending on the outcome of this test, a bond is formed or not. This process is repeated until the value of each point of the lattice corresponding to a saturated center or an "equilibrium" condition is detected. The probability factors are varied to fit the experimental data (Figure 3). In Table II one finds the relative probabilities derived from the lattice model and used to provide the fit of Figure 3 (a coordination number of 26 was assumed for this particular solution; see the discussion below). The uniqueness of the solution where such a large number of parameters are varied appears at a first glance to be problematic, but that this is not a concern becomes apparent when one examines the corresponding set of differential equations which one can write for the reactions of Scheme I. Several of the constants (e.g., p_4, p_5, p_6 in the expression for M*) are exactly zero. This fact coupled with knowledge of initial conditions make the system tractable. The experimental accuracy itself becomes a more important consideration. The total integrated area should remain a constant over the course of the experiment. In fact, over a series of experiments the standard deviation of this quantity ranged from 1.9% to 3.7%. The question that one next asks is how this error is distributed over the resonances. This is more difficult to answer, but it is likely that the largest errors reside in the integration of the rather broad envelop of peaks associated with MID and SAT groups. Constants appearing in the expressions for these entities may have as much as 25% error associated with them. This is estimated by assuming the total error is in the integrated value for the SAT or MID functionality (whichever error is larger) and then determining the deviation over the course of the experiment. At low concentrations of a MID or SAT species, the error is quite large simply because of the small amount of signal.

The sensitivity of the solution to the lower probability events, p_5 and p_6, was interrogated by comparison of long-term data where one would anticipate the most pronounced dependence. The departure of the solution optimized for time <2 h from longer time was interpreted as evidence for a reversible process involving MID and SAT groups. This reversibility was not accounted for in the model described in this paper, although preliminary efforts to incorporate limited reversibility suggest that, at least mathematically, one can improve the fit dramatically by assuming an equilibrium in place of reaction 6. We feel the data are not precise enough to warrant such a treatment. Therefore, for the purposes of this discussion, the condensation of trifunctional siloxanes is considered to be an irreversible reaction sequence.

As alluded to above, the concept of a neighborhood implicitly provides another variable that must be accounted for in the modeling process. One might suppose that this value is related to the coordination number of the center of interest; however, as this is a kinetic model, the neighborhood is the integrated coordination states of a reactive center determined during its lifetime between reactions. From the hydrolysis studies one can estimate the rate constants for the condensation to be approximately 10^{-2} to 10^{-3} M^{-1} s^{-1}, suggesting 10^{12} to 10^{14} collisions between reactions.[16] The neighborhood would seem to be very large.

To investigate the coordination number (CN) dependency, two extreme scenarios were assumed. The first of these had a small neighborhood ranging from the physically meaningful sizes 12-, 8-, or 6-coordination to a 26-coordinate arrangement—an unattainable packing in three-space. In each configuration, all sites were considered to be equivalent. For the CN = 26 case, the probabilities of Table II yield the fit of Figure 3. One sees little discrimination between the most rapid and slowest process (about an order of magnitude). In the cases of CN = 6, 8, or 12, the overall time constant for array development increases with lower CN, but relative probabilities remain unchanged. Qualitatively, the fit improves as one goes to large CN. Indeed, in the case of CN = 6, the neighborhoods become depleted and the fit becomes very poor.

The other extreme was a large neighborhood spanning the entire array (8000 points). The probabilities (Table II) have not only diverged (almost 3 orders of magnitude), but the relative ordering has changed. Whether this is a limiting solution or yet larger arrays were incorporated the continued divergence would seem addressable in at least two ways. One could use larger and larger arrays. As computing time was already a limiting factor, this approach was deemed less palatable than the alternative. To this end a set of difference equations describing the reaction sequence was solved and yielded the rate constants listed in Table III. The relative magnitudes of these constants are also included in Table II. Rather than making arguments based on small differences in the various rate con-

Table III
Rate Constants for Condensation[a]

n	k_n, M^{-1} s^{-1}	n	k_n, M^{-1} s^{-1}
1	6.9×10^{-3}	4	7.5×10^{-4}
2	1.0×10^{-2}	5	2.8×10^{-4}
3	1.5×10^{-3}	6	1.5×10^{-5}

[a] Determined at calculated pH 2.85 (22 °C). Compare with MTMS hydrolysis at pH 3.0 in acetone/water (30 °C): $k_{obsd} = 6.4 \times 10^{-3}$ M^{-1} s^{-1}.

stants, a decomposition of the results into propagation and other condensation processes is instructive. A comparison of $\bar{k}_{prop}$ ($\bar{k}_{prop} \equiv {}^1/_3\sum_{i=1}^{3} k_i$) versus $\bar{k}_{cond}$ ($\bar{k}_{cond} \equiv {}^1/_3\sum_{i=4}^{6} k_i$) from the lattice and the difference equations shows the relative magnitudes are similar, $\bar{s}_{prop} = 16\bar{s}_{cond}$ compared with $\bar{k}_{prop} = 17\bar{k}_{cond}$. These data suggest that larger arrays would produce results not significantly different from those obtained with the 8K array; although, the functional dependence of array size to probability values needs to be examined in detail.

In the case where one is treating the entire array as a neighborhood, the model, a multinominal distribution, can be simply represented by the following: P(reaction at rth cycle) = $s_k p_i p_j$, where s_k are the scalar test values associated with the six processes considered in the model and, for example, $p_i = n_i/N$ with n_i being the number of i centers in the array of size N. The values, n_i, are conditional on P(reaction at the $(r-1)$th cycle) and so forth.[17] This situation can be expressed in the following fashion as a Markov process:

$$\begin{pmatrix} p_{M\bullet} \\ p_{END} \\ p_{MID} \\ p_{SAT} \end{pmatrix}_t \hat{\mathbf{T}} = \begin{pmatrix} p_{M\bullet} \\ p_{END} \\ p_{MID} \\ p_{SAT} \end{pmatrix}_{t+1}$$

where the transition matrix, $\hat{\mathbf{T}}$, equals

$$\begin{pmatrix} 1 - T(1,2) & T(1,2) & 0 & 0 \\ 0 & 1 - T(2,3) & T(2,3) & 0 \\ 0 & 0 & 1 - T(3,4) & T(3,4) \\ 0 & 0 & 0 & 1 \end{pmatrix}$$

with, for example, $T(1,2) = s_1 p_{M\bullet}{}^t + s_2 p_{END}{}^t + s_3 p_{MID}{}^t$ and $p_x{}^t$ being the probability of picking species x at time t. Clearly, this expression on expansion yields the same set of equations as obtained by reducing the reaction sequence to its differential form. Some license has been taken in equating the discrete form with the continuous representation, but since the differential equations were solved as difference equations, this subtlety can be overlooked.

In the above treatment, s_i are equivalent to k_i. In the event where small neighborhoods are assumed the relationship of the two sets of constants is obscure.

Attributes of the Lattice Model. Given that one can deduce event probabilities which are related in some (albeit, unknown) fashion to reaction rate constants, what does the lattice model give us that the difference equations do not?

By characterizing the species formed during the modeling, one can determine molecular weight distributions (Figure 4) as well as gel points. The gel point determined in this fashion is defined to be the point of greatest change in the maximum molecular weight species, ΔMW_{max}, as a function of extent of reaction, p. A plot (Figure 5) of this function using the parameters of Table II (CN = 26) shows the gel point occurring at 67% reaction. With the large coordination number (8K) and the corresponding probabilities of Table II, the gel point is determined to be 61.53 ± 0.09% (five realizations).

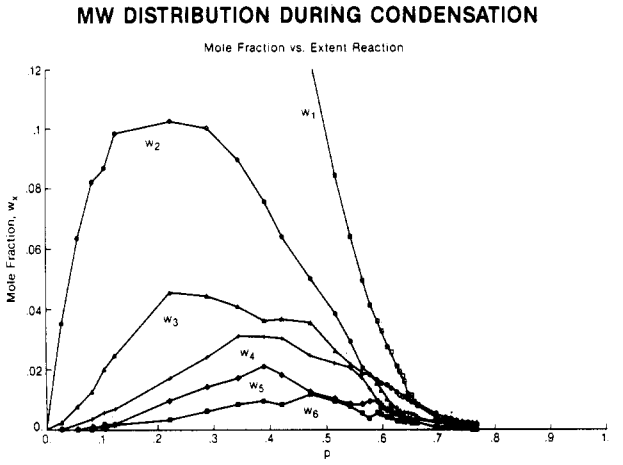

Figure 4. Calculated distribution of oligomeric species as function of reaction; CN = 26, probabilities from Table II.

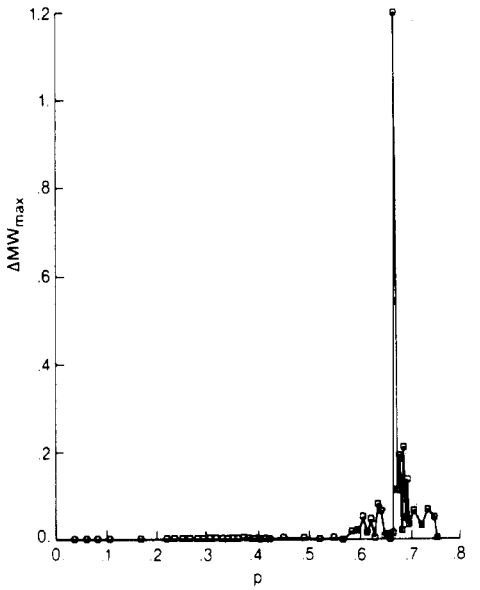

Figure 5. Change of the maximum molecular weight oligomer as a function of extent of reaction; CN = 26, probabilities from Table II.

Experiments to determine MW distributions in these systems have not yet been successfully carried out. Determinations of the gel point also is problematic in that with proton catalysts at the concentrations necessary to conveniently monitor the reaction, gel formation is not observed. With certain Lewis acid catalysts gels are formed from MTMS hydrolysis, but the absence of reversibility of certain siloxane bond formation with these catalysts could explain this difference.[18] An alternative explanation may arise from the work of Coniglio.[19] The effect of solvent is not treated in the simple model described here and certainly may effect gelation. Therefore at this time, one is left with the far less satisfying possibility of comparing this model to other treatments.

In F–S theory all functionalities of a multifunctional monomer were considered to have equal reactivity. By ascribing equal values to the probability factors of the lattice model, one determines the gel point to take place at 50% reaction for CN = 26. In the case of CN = 8K and all probabilities equal, the gel point is determined to be 43.3 ± 0.1% (four realizations). A more interesting comparison is the shape of the function ($\Delta MW_{max}(p)$) with a spectrum of probabilities (reactivities) versus all equal

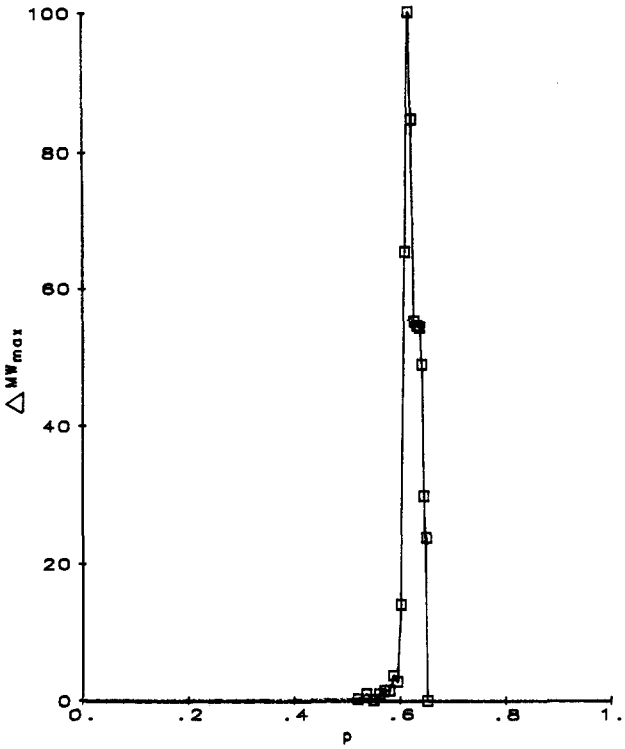

Figure 6. Change of the maximum molecular weight oligomer as a function of extent of reaction; CN = 8K, probabilities from Table II.

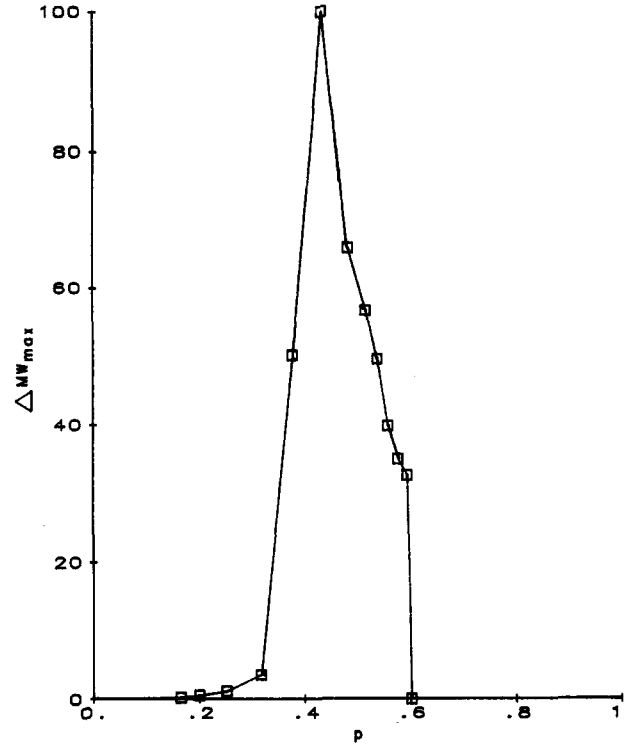

Figure 7. Change of the maximum molecular weight oligomer as a function of extent of reaction; CN = 8K, equal probabilities.

probabilities. The sharp transition ($w_{1/2} \leq 0.02$) observed in the case where there is a spectrum of reactivities (i.e., Figure 5 or 6) is replaced with a broad, poorly defined change ($w_{1/2} = 0.18$ in Figure 7). F–S theory predicts the gel point at 50% reaction.[10] The lattice treatment of de Gennes predicts a gel point at 63% reaction.[14a] Neither approach characterizes the change. The physical interpretation of this observation may simply mean that a uniform development of MW leads to a fuzzy transition, whereas a lumpy early distribution evolves through a sharp transition point in which bonds crucial to large MW change are derived from lower probability events.

Conclusions

The hydrolysis of methyltrimethoxysilane in an acetone/water solvent system was found to be competitive with condensation of partially hydrolyzed methoxysilane. To the extent one can compare this system with tetraalkoxysilane hydrolysis and condensation, this finding differs from the conclusion of other workers[2e] who have dissected the hydrolysis and condensation processes into two regimes having a 12-fold rate difference. Indeed, the data of Assink et al. should probably be viewed as hydrolysis and condensation of partially hydrolyzed monomer in the initial more rapid process, followed by slower condensation reactions not involving monomeric species. The rate difference ascribed to the two types of reactions is consistent with our data.

Has our attempt to derive a statistical model from kinetics considerations with no accounting for structure, and thus implicitly the thermodynamics associated with structure, any merit? The lattice models currently in the literature account for structure from the onset of percolation.[14] That is, structures found in the products are imposed as the system evolves. The data in our particular system cannot be modeled with these structural constraints (in our scheme, coordination numbers of 12 or less). In addition, at higher coordination numbers (CN = 26), the fit, although good (numerically speaking), does not correspond to the kinetics of the system. It follows that the current literature models may not model percolation at times before gel if kinetics dictates events. To the extent that the kinetics of a process reflects the thermodynamics the structurally based models should account for the entire condensation to gelation process. By the same argument the kinetic model should likewise produce an accurate description. The problem apparently lies in the particular system being investigated—one that has both kinetic and thermodynamic controls operating simultaneously. In the next stage of modeling, one must account for both factors. Proper tests of such models should be the evolution of finite species, as well as the appearance of critical points and structure.

Experimental Section

Methyltrimethoxysilane was obtained from Silar and distilled from sodium and sodium methoxide. Acetone (Aldrich Gold Label) was used as received. Water was distilled and passed through a series of millipore filters and an activated carbon bed. *n*-Decane (Aldrich) was used as received as an internal standard in GC analysis. The GC analysis was performed on a Shimadzu GC-9A with C-R1B data analyzer. TC detection in conjunction with a 6-ft 3% OV-101 column was used. Temperatures were maintained to ±0.2 °C in a circulating water bath equipped with a Thermomix heater/circulator.

NMR analyses were carried out on either a Varian 200 (observed frequency for ^{29}Si, 39.75 MHz) or 300 MHz (59.59 MHz) FTNMR spectrometer at 20–22 °C.

Computational work was performed on a VAX 11-780 using utilities of the VMS system. Long-time development of the lattice typically ran to (1.5–2.0) × 10^6 cycles. No methods to limit sampling unproductive array points were incorporated; although, such techniques are currently being investigated.

Kinetics by GC Analysis. A typical procedure is as follows: A 100.0-mL acetone solution containing 1.50 g (final concentration = 0.109 M) of methyltrimethoxysilane, 0.5 g of decane, and 2.0 mL of water was placed into a bath and allowed to equilibrate for at least one hour. To this solution was added 1.0 mL of a 3.2 × 10^{-3} M solution of *p*-toluenesulfonic acid in acetone. The concentration of the stock *p*-TSA solution was determined by titration with standard base to a phenolphthalein end point. The

reaction mixture was shaken virogously to achieve mixing and sampled until the concentration of substrate was below the detection limits of the GC.

NMR Experiments. A typical NMR experiment was performed as follows: A solution of methyltrimethoxysilane (1.0 g, 7.3 mM) in acetone-d_6 (2.0 mL) was placed into a NMR tube along with 25–35 mg of $Cr(acac)_3$. Water (0.40 mL) was added by syringe. A spectrum of this solution was obtained and remained unchanged with time. Addition of the catalyst (0.050 mL of a 6.8×10^{-2} M solution of *p*-TSA in acetone) was followed by rapid mixing and acquisition of spectra over several hours.

Acknowledgment. I express my thanks to E. Williams, J. Smith, and P. Donahue for technical assistance. Also, useful discussions with J. T. Bendler and F. Faltin are appreciated.

Registry No. $H_3CSi(OCH_3)_3$, 1185-55-3.

References and Notes

(1) (a) For a review of hydrolysis, see: Prince, R. H. In *M. T. P. International Reviews of Science Inorganic Series One*; Tobe, M. L., Ed.; Butterworths: London, 1972; Vol. 9. (b) Smith, K. A. *J. Org. Chem.* **1986**, *51*, 3827 and references cited therein.
(2) (a) Engelhardt, G.; Altenburg, W.; Hoebbel, D.; Wieker, W. *Z. Anorg. Allg. Chem.* **1977**, *428*, 43. (b) Harris, R. K.; Newman, R. H. *J. Chem. Soc., Faraday Trans. 2* **1977**, *73*, 1204. (c) Harris, R. K.; Knight, C. T. G.; Smith, D. N. *J. Chem. Soc., Chem. Commun.* **1980**, 726. (d) Lin, C. C.; Basil, J. D. *Mater. Res. Soc. Symp. Proc.* **1986**, *73* (Better Ceramics through Chemistry), 585. (e) Assink, R. A.; Kay, B. D. *Mater. Res. Soc. Symp. Proc.* **1984**, *32* (Better Ceramics through Chemistry), 301. (f) *Ultrastructure Processing of Ceramics, Glasses, and Composites*; Hench, L. L., Ulrich, D. R., Eds.; Wiley-Interscience: New York, 1984.
(3) Noll, W. *Chemistry and Technology of Silicones*; Academic: New York, 1968.
(4) (a) Brown, J. F.; Vogt, Jr., L. H. *J. Am. Chem. Soc.* **1965**, *87*, 4313. (b) Pohl, E. R.; Osterholtz, F. D. In *Silanes, Surfaces and Interfaces*; Leyden, D. E., Ed.; Gordon and Breach: New York, 1986; Vol. 1 of series on Chemically Modified Surfaces, p 481.
(5) Hanneman, L. F. In *Analysis of Silicones*, Smith, A. L., Ed.; Krieger: Malabar, FL, 1983; p 234.
(6) Gordon, A. J.; Ford, R. A. *The Chemists Companion*; Wiley: New York, 1972; p 61. (b) Bausch, M.; Bordwell, F., personal communication.
(7) Paul, M. A.; Long, F. A. *Chem. Rev.* **1957**, *57*, 1–45.
(8) Since relaxation of the various silicons in the sample was promoted by the addition of $Cr(acac)_3$ and all the silicons reside in essentially the same ligand field, namely, three oxygens and one carbon, the integrated areas are representative of the relative amounts of each silicon. See: Levy, G. C.; Cargioli, J. D.; Juliano, P. C.; Mitchell, T. D. *J. Am. Chem. Soc.* **1973**, *95*, 3445–3454.
(9) Marsmann, H. In *NMR Basic Principles and Progress Grundlagen and Fortschritte*; Diehl, P., Fluck, E., Kosfeld, R., Eds.; Springer-Verlag: Berlin, 1981; Vol. 17, pp 184–185.
(10) Flory, P. J. In *Frontiers in Chemistry Series*; Grummett, O., Burk, R. E., Eds.; Interscience: New York, 1949; Vol. VI, pp 263–282 and references cited therein.
(11) Stockmayer, W. H. *J. Chem. Phys.* **1943**, *11*, 45.
(12) Stauffer, D.; Coniglio, A.; Adam, M. *Adv. Polym. Sci.* **1982**, *44*, 103.
(13) (a) Good, I. J. *Proc. Cambridge Philos. Soc.* **1948**, *45*, 360. (b) Gordon, M. *Proc. R. Soc. London*, A **1962**, *268*, 240.
(14) (a) de Gennes, P.-G. *J. Phys. Lett.* **1976**, *37*, L1. (b) Herrmann, H. J.; Stauffer, D.; Landau, D. P. *J. Phys. A: Math. Gen.* **1983**, *16*, 1221–1239. (c) Orbach, R. *Science (Washington, D.C.)* **1986**, *231*, 814–819 and references cited therein.
(15) Bruns, W.; Motoc, I.; O'Driscoll, K. F. In *Monte-Carlo Applications in Polymer Science*; Springer-Verlag: Heidelberg, 1981; Lecture Notes in Chemistry 27.
(16) This assumes that the mean half-life between collisions is approximately the same magnitude as would be expected for a solute diffusing between sites.
(17) Ethier, S. N.; Kurtz, T. G. In *Markov Processes Characterization and Convergence*; Wiley: New York, 1986; "Density Dependent Population Processes".
(18) Smith, K. A., unpublished results.
(19) Coniglio, A.; Stanley, H. E.; Klein, W. *Phys. Rev. Lett.* **1979**, *42*, 518.

Excluded-Volume Effects in Rubber Elasticity. 1. Virial Stress Formulation[1]

J. Gao and J. H. Weiner*

Department of Physics and Division of Engineering, Brown University, Providence, Rhode Island 02912. *Received March 12, 1987; Revised Manuscript Received June 10, 1987*

ABSTRACT: The usual view of stress in rubber elasticity focuses upon the axial force in the component chains as giving rise to stress across an arbitrary interior plane. The virial stress formulation provides a more local view of the stress in a rubber-like system in which both the covalent interactions responsible for the chain bonds and the noncovalent interactions appear on an equal footing. This formulation is applied here to a chain with excluded volume. It is shown that the virial viewpoint corresponds to considering forces across fixed spatial planes and therefore requires inclusion of momentum transport. By contrast, the usual approach treats forces between fixed sets of atoms and momentum transport does not enter. The equivalence of the two viewpoints is demonstrated.

Introduction

From the viewpoint of the thermal motion of its atoms, a rubberlike material occupies a position intermediate between a glassy solid and a fluid. The long-time average positions of its atoms are approximately uniformly distributed in space as is the case for a glassy solid, but the amplitudes of their thermal motion about these mean positions are much larger. One would therefore expect that the atomic interpretation of stress should share features of that for a glass, for which the interatomic forces exerted across an arbitrary internal plane play the primary role, and that for a fluid where momentum transfer becomes important.

The usual view of stress in rubber elasticity, however, bypasses both viewpoints and focuses upon the axial force in the component chains as giving rise to the stress across an arbitrary interior plane. Noncovalent interactions, including those due to excluded volume, are generally not

0024-9297/87/2220-2520$01.50/0